

NJC

Accepted Manuscript



This is an *Accepted Manuscript*, which has been through the Royal Society of Chemistry peer review process and has been accepted for publication.

Accepted Manuscripts are published online shortly after acceptance, before technical editing, formatting and proof reading. Using this free service, authors can make their results available to the community, in citable form, before we publish the edited article. We will replace this *Accepted Manuscript* with the edited and formatted *Advance Article* as soon as it is available.

You can find more information about *Accepted Manuscripts* in the [Information for Authors](#).

Please note that technical editing may introduce minor changes to the text and/or graphics, which may alter content. The journal's standard [Terms & Conditions](#) and the [Ethical guidelines](#) still apply. In no event shall the Royal Society of Chemistry be held responsible for any errors or omissions in this *Accepted Manuscript* or any consequences arising from the use of any information it contains.

For submission to *New J. Chem.* Revised Manuscript (NJ-ART-07-2015-001708)

Synthesis, Structures and Magnetism of series of Binuclear and one-dimensional Ni-Ln Complexes: Single-molecule Magnetic Behavior in one-dimensional Nitrate-bridged Dy Analogue

Min-Xia Yao,* Xing-Yun Lu, Zhao-Xia Zhu, Xiao-Wei Deng, and Su Jing*

College of Chemistry and Molecular Engineering, Nanjing Tech University, Nanjing, 211816, P. R. China.

Abstract

By diffusion of methyl *tert*-butyl ether vapor into the acetonitrile solution containing $[\text{Ni}(\text{L})(\text{H}_2\text{O})_2]$ ($\text{L} = 1,2\text{-bis}(3\text{-methoxy-salicylideneaminoxy})\text{ethane}$) and $\text{Ln}(\text{NO}_3)_3 \cdot 6\text{H}_2\text{O}$, three Ni-Ln heterometallic complexes, $[\text{Ni}(\mu\text{-L})(\text{MeCN})_2\text{Ln}(\text{NO}_3)_3]$ ($\text{Ln} = \text{Gd}$ for **1**, Tb for **2**), and $[\text{Ni}(\mu\text{-L})(\text{MeCN})\text{Dy}(\text{NO}_3)_2(\mu\text{-NO}_3) \cdot \text{MeCN}]_n$ (**3**) had been obtained. When the reaction was carried out in methanol/chloroform (2:1) containing H_2L , $\text{Ni}(\text{Ac})_2 \cdot 4\text{H}_2\text{O}$ and $\text{Ln}(\text{NO}_3)_3 \cdot 6\text{H}_2\text{O}$ with diethyl ether vapor diffused, two Ni-Ln heterometallic complexes $[\text{Ni}(\mu\text{-L})(\text{CH}_3\text{OH})(\mu\text{-NO}_3)\text{Ln}(\text{NO}_3)_2]$ ($\text{Ln} = \text{Tb}$ for **4**, and Dy for **5**) had been synthesized. The X-ray analyses demonstrated that complexes **1**, **2**, **4** and **5** display 3d-4f heterobinuclear structures, Ni^{II} and Ln^{III} ions are bridged by diphenolato atoms for **1** and **2**, and by an *syn-syn* nitrate group and diphenolato atoms for **4** and **5**. Compound **3** is made up of a rare *anti-anti* nitrate- and phenolate-bridged Ni–Dy heterometallic chain. All complexes exhibit net ferromagnetic interaction between Ni^{II} and Ln^{III} ions. Alternating current susceptibility measurements demonstrated that compound **3** behaved as a single-molecule magnet with the effective energy barriers of 15.8 K under zero direct current field, however, **5** only displays the slow magnetic relaxation under 2000 Oe direct current field.

* To whom correspondence should be addressed. Email: yaomx@njtech.edu.cn ; sjing@njtech.edu.cn. Fax: +86-25-58139528. Nanjing Tech University.

Introduction

Molecule-based magnetic materials involving chemistry, physics, and material science have attracted more and more attention, some of which behave as single-molecule magnets (SMMs) or single-chain magnets (SCMs) that possess an energy barrier (U_{eff}) to the inversion of the magnetic moment, resulting in slow relaxation of the magnetization below a blocking temperature (T_B), and have been proposed as candidates for applications in high-density information storage, molecular spintronics and quantum computation.¹⁻⁵ To a SMM, it must possess a large spin ground state (S), high uniaxial magnetic anisotropy (D), and negligible intercluster magnetic interactions. For a single-chain magnet (SCM), a large magnetic anisotropy of spin carriers and strong intrachain magnetic couplings are essential.¹⁻³

Since the first mixed 3d-4f SMM, Cu_2Tb_2 , was reported in 2004,⁶ many 3d and 4f heterometal complexes have been synthesized for the sake of increasing the height of the energy barrier and improving the T_B of SMM/SCMs.⁷ In these complexes, 3d ions such as Co^{II} , Ni^{II} , Mn^{III} and Fe^{III} can give rise to stronger magnetic coupling and/or magnetic anisotropy, and lanthanide (Ln) ions, especially Dy^{III} , Tb^{III} , Ho^{III} , and so forth, which have a large ground-state spin and a strong easy axis magnetic anisotropy strongly susceptible to the symmetry of the ligand field, contribute large Ising-type magnetic anisotropy.⁸ Moreover, the magnetic coupling of the heavy lanthanide ions with 3d ions is often ferromagnetic, which leads to ground states with even larger magnetic moments.⁹ However, due to the fast quantum tunnelling of magnetization (QTM) between ground states for anisotropical Ln ions, the most of these reported complexes exhibit field-induced SMM behaviors,¹⁰⁻¹³ only a few behave as SMMs under zero dc field.¹⁴ A few SCMs by introducing organic radical molecules or paramagnetic metalloligands as spacer have been reported.^{9c,15} It has been proved that the QTM effect can be suppressed by raising the symmetry of the ligand-field around Ln ions, such as the well-known quasi- D_{5h} , D_{4d} and C_3 configuration, and/or strengthening the magnetic couplings between 3d and 4f ions.¹⁶

Here, in order to further understand and improve 3d-4f heterometallic SMM/SCMs behaviors, we synthesized series of Ni-Ln heterometallic complexes by using the oxime-based Salen-type compartmental ligand (L) belonging to diphenolato bridges that can transmit the strongest magnetic coupling between 3d and 4f ions, $[\text{Ni}(\mu\text{-L})(\text{MeCN})_2\text{Ln}(\text{NO}_3)_3]$ (Ln = Gd for **1**, Tb for **2**, respectively),

$[\text{Ni}(\mu\text{-L})(\text{MeCN})\text{Dy}(\text{NO}_3)_2(\mu\text{-NO}_3)\cdot\text{MeCN}]_n$ (**3**), and $[\text{Ni}(\mu\text{-L})(\text{CH}_3\text{OH})(\mu\text{-NO}_3)\text{Ln}(\text{NO}_3)_2]$ (Ln = Tb for **4**, and Dy for **5**, respectively). Their crystal structures and magnetic properties were investigated. Due to the different symmetry of the ligand-field around Dy^{III} ions, the one-dimensional (1D) chain polymer of **3** behaves as a SMM under zero direct current (dc) field, and the binuclear compound of **5** exhibits field-induced slow magnetic relaxation. To our knowledge, compound **3** is an unique example of 1D infinite nitrate- and phenolate-bridged Ni–Dy heterometallic chain.

Experimental

Starting materials

All the reagents were commercially available and used without further purification. The H₂L and [Ni(L)(H₂O)₂] was synthesized following a published method.¹⁷

Caution: Although no problems were encountered in this work, the diethyl ether is potentially explosive. Thus, these starting materials should be handled in small quantities and with great care.

Syntheses

Preparation of [Ni(μ-L)(MeCN)₂Gd(NO₃)₃] (**1**)

A solution of [Ni(L)(H₂O)₂] (18.1 mg, 0.04 mmol) in acetonitrile (2 mL) was added to a solution of Gd(NO₃)₃·6H₂O (18 mg, 0.04 mmol) in 2 mL of acetonitrile, resulting in immediate formation of a green solution. Diffusion of methyl *tert*-butyl ether vapor into this solution produced purple block crystals of **1**. Yield: 58%. Anal. Calcd for C₂₂H₂₄GdN₇NiO₁₅: C 31.37, H 2.87, N 11.64. Found: C 31.65, H 2.69, N 11.88. IR (KBr, cm⁻¹): 1610 (ν_{C=N}), 1384 (ν_{NO₃⁻}).

Preparation of [Ni(μ-L)(MeCN)₂Tb(NO₃)₃] (**2**)

Compound **2** was prepared as purple block crystals in a similar method to that of **1**, except that Tb(NO₃)₃·6H₂O was used. Yield: 60%. Anal. Calcd for C₂₂H₂₄TbN₇NiO₁₅: C 31.30, H 2.86, N 11.62. Found: C 31.62, H 2.63, N 11.93. IR (KBr, cm⁻¹): 1611 (ν_{C=N}), 1384 (ν_{NO₃⁻}).

Preparation of [Ni(μ-L)(MeCN)Dy(NO₃)₂(μ-NO₃)·MeCN]_n (**3**)

Compound **3** was prepared as purple block crystals in a similar method to that of **1**, except that Dy(NO₃)₃·6H₂O was used. Yield: 63%. Anal. Calcd for C₂₂H₂₄DyN₇NiO₁₅: C 31.17, H 2.85, N 11.57. Found: C 31.09, H 3.07, N 11.78. IR (KBr, cm⁻¹): 1610

($\nu_{C=N}$), 1384 ($\nu_{NO_3^-}$).

Preparation of [Ni(μ -L)(CH₃OH)(μ -NO₃)Tb(NO₃)₂] \cdot Et₂O (4)

A solution of H₂L (21.6 mg, 0.06 mmol) in methanol/chloroform (v/v = 2:1) (2 mL) was added to a solution of Ni(Ac)₂ \cdot 4H₂O (14.9 mg, 0.06 mmol) in 2 mL of methanol/chloroform (v/v = 2:1), then Tb(NO₃)₃ \cdot 6H₂O (26.1 mg, 0.06 mmol) in 2 mL of methanol/chloroform (v/v = 2:1) was added, resulting in immediate formation of a green solution. Diffusion of diethyl ether vapor into this solution produced green block crystals of **4**. Yield: 55%. Anal. Calcd for C₂₃H₃₂TbN₅NiO₁₇: C 31.82, H 3.71, N 8.07. Found: C 32.17, H 3.38, N 8.23. IR (KBr, cm⁻¹): 1608 ($\nu_{C=N}$), 1380 ($\nu_{NO_3^-}$).

Preparation of [Ni(μ -L)(CH₃OH)(μ -NO₃)Dy(NO₃)₂] \cdot Et₂O (5)

Compound **5** was prepared as purple block crystals in a similar method to that of **4**, except that Dy(NO₃)₃ \cdot 6H₂O was used. Yield: 57%. Anal. Calcd for C₂₃H₃₂DyN₅NiO₁₇: C 31.69, H 3.70, N 8.03. Found: C 31.54, H 3.57, N 8.28. IR (KBr, cm⁻¹): 1608 ($\nu_{C=N}$), 1380 ($\nu_{NO_3^-}$).

X-ray Structure Determination. The crystal structures were determined on a Siemens (Bruker) SMART CCD diffractometer using monochromated Mo $K\alpha$ radiation ($\lambda = 0.71073$ Å) at 292 K. Cell parameters were retrieved using SMART software and refined using SAINT¹⁸ on all observed reflections. Data was collected using a narrow-frame method with scan widths of 0.30° in ω and an exposure time of 10 s/frame. The highly redundant data sets were reduced using SAINT¹⁸ and corrected for Lorentz and polarization effects. Absorption corrections were applied using SADABS¹⁹ supplied by Bruker. Structures were solved by direct methods using the program SHELXL-2013.²⁰ The positions of the metal atoms and their first coordination spheres were located from direct-methods E maps; other non-hydrogen atoms were found in alternating difference Fourier syntheses and least-squares refinement cycles and, during the final cycles, refined anisotropically. Hydrogen atoms were placed in calculated positions and refined as riding atoms with a uniform value of U_{iso} which are tied 1.2 times or 1.5 times (for methyl- group) to the parent atoms. Final crystallographic data and values of R_1 and wR_2 are listed in Table 1. Selected bond distances and angles for complexes **1–5** are listed in Tables S1–5.

CCDC reference numbers 1408411 (**1**), 1408412 (**2**), 1408413 (**3**), 1408414 (**4**), and 1408415 (**5**).

Table 1 Summary of crystallographic data for the complexes **1–5**

	1	2	3	4	5
formula	C ₂₂ H ₂₄ GdN ₇ Ni O ₁₅	C ₂₂ H ₂₄ TbN ₇ Ni O ₁₅	C ₂₂ H ₂₄ DyN ₇ Ni O ₁₅	C ₂₃ H ₃₂ TbN ₅ Ni O ₁₇	C ₂₃ H ₃₂ DyN ₅ Ni O ₁₇
fw	842.44	844.11	847.69	868.16	871.74
crystal system	Monoclinic	Monoclinic	Monoclinic	Triclinic	Triclinic
space group	<i>P</i> 2 ₁ / <i>n</i>	<i>P</i> 2 ₁ / <i>n</i>	<i>Cc</i>	<i>P</i> ₋₁	<i>P</i> ₋₁
<i>a</i> , Å	10.3265(19)	10.309(3)	21.577(3)	10.0281(14)	10.0241(17)
<i>b</i> , Å	17.115(3)	17.095(5)	9.4531(12)	12.0551(17)	12.042(2)
<i>c</i> , Å	17.194(3)	17.232(5)	15.866(2)	15.254(2)	15.270(3)
<i>a</i> , deg	90.00	90.00	90.00	71.779(2)	71.869(2)
<i>β</i> , deg	96.575(3)	96.548(4)	114.880(2)	86.572(2)	86.592(3)
<i>γ</i> , deg	90.00	90.00	90.00	68.175(2)	68.157(2)
<i>V</i> , Å ³	3018.8(10)	3017.2(14)	2935.9(6)	1622.7(4)	1622.6(5)
<i>Z</i>	4	4	4	2	2
ρ_{calcd} , g cm ⁻³	1.854	1.858	1.918	1.777	1.784
<i>T</i> / K	296(2)	296(2)	296(2)	296(2)	296(2)
μ , mm ⁻¹	2.884	3.031	3.251	2.823	2.946
θ , deg	1.68t o 26.00	1.68 to 26.00	2.08 to 25.99	1.401to 26.00	1.92 to 26.00
<i>F</i> (000)	1668	1672	1676	868	870
index ranges	-12<= <i>h</i> <=12 -21<= <i>k</i> <=21 -21<= <i>l</i> <=19	-12<= <i>h</i> <=12 -21<= <i>k</i> <=11 -21<= <i>l</i> <=21	-26 ≤ <i>h</i> ≤ 26 -11 ≤ <i>k</i> ≤ 10 -17 ≤ <i>l</i> ≤ 19	-12<= <i>h</i> <=12 -14<= <i>k</i> <=14 -18<= <i>l</i> <=17	-8 ≤ <i>h</i> ≤ 12 -14 ≤ <i>k</i> ≤ 14 -18 ≤ <i>l</i> ≤ 18
data/restraints /parameters	5918 / 0 / 420	5935 / 6 / 420	4915/ 2/ 420	6270/1/429	6278/1/429
GOF (<i>F</i> ²)	1.074	1.104	0.874	1.023	0.904
<i>R</i> ₁ ^{<i>a</i>} , <i>wR</i> ₂ ^{<i>b</i>} (<i>I</i> >2σ(<i>I</i>))	0.0287 0.0736	0.0202 0.0495	0.0153 0.0354	0.0318 0.0891	0.0379 0.1062
<i>R</i> ₁ ^{<i>a</i>} , <i>wR</i> ₂ ^{<i>b</i>} (all data)	0.0326 0.0758	0.0245 0.0508	0.0160 0.0357	0.0350 0.0911	0.0428 0.1108

$$R_1^a = \frac{\sum ||F_o| - |F_c||}{\sum F_o}, \quad wR_2^b = \left[\frac{\sum w(F_o^2 - F_c^2)^2}{\sum w(F_o^2)^2} \right]^{1/2}$$

Physical Measurements. Elemental analyses for C, H and N were performed on a Perkin-Elmer 240C analyzer. Infrared spectra were recorded on a Vector22 Bruker Spectrophotometer with KBr pellets in the 400–4000 cm⁻¹ region. Magnetic susceptibilities for all polycrystalline samples embedded in eicosane were measured with the use of a Quantum Design MPMS-XL7 SQUID magnetometer in the temperature range 1.8–300 K. Field dependences of magnetization were measured

using Quantum Design MPMS-XL5 SQUID system in an applied field up to 50 kOe. All data were corrected for diamagnetism of the eicosane, the sample holder, and the constituent atoms using Pascal's constants.

Results and discussion

Synthesis and general characterization

Complexes **1–3** were synthesized and crystallized from the reaction mixture containing $[\text{Ni}(\text{L})(\text{H}_2\text{O})_2]$ and $\text{Ln}(\text{NO}_3)_3 \cdot 6\text{H}_2\text{O}$ in a 1:1 molar ratio in an acetonitrile solution at room temperature. Diffusion of methyl *tert*-butyl ether vapor into the above solution produced purple block crystals. The single crystal X-ray analyses confirmed the structure of $[\text{Ni}(\mu\text{-L})(\text{MeCN})_2\text{Ln}(\text{NO}_3)_3]$ ($\text{Ln} = \text{Gd}$ for **1**, Tb for **2**, respectively), and $[\text{Ni}(\mu\text{-L})(\text{MeCN})\text{Dy}(\text{NO}_3)_2(\mu\text{-NO}_3)\cdot\text{MeCN}]_n$ (**3**). Elemental analyses agreed with the above chemical formula. The IR spectra showed also a characteristic band at 1610 cm^{-1} assignable to a C=N stretching vibration of the Schiff-base ligand and the strong absorptions at 1384 cm^{-1} , due to the presence of the nitrate groups. Complexes **4** and **5** were similarly synthesized in an methanol/chloroform (v/v = 2:1) solution by mixing H_2L , $\text{Ni}(\text{Ac})_2 \cdot 4\text{H}_2\text{O}$ and $\text{Ln}(\text{NO}_3)_3 \cdot 6\text{H}_2\text{O}$ in a 1:1:1 molar ratio at room temperature. Diffusion of diethyl ether vapor into the above solution produced green block crystals. The single crystal X-ray analyses confirmed the structure of $[\text{Ni}(\mu\text{-L})(\text{CH}_3\text{OH})(\mu\text{-NO}_3)\text{Ln}(\text{NO}_3)_2]$ ($\text{Ln} = \text{Tb}$ for **4**, and Dy for **5**, respectively). Elemental analyses agreed with the above chemical formula. Complexes **4** and **5** also exhibits characteristic IR bands, similar to those observed for **1–3**. It should be noted that when the reaction solvent were changed, the distinct structure were exhibited for complexes **1-5**.

Structural Description.

Compounds **1** and **2** are isostructural, crystallize in the monoclinic space group $P2_1/n$ and consist of one neutral $[\text{Ni}(\mu\text{-L})(\text{MeCN})_2\text{Ln}(\text{NO}_3)_3]$ ($\text{Ln} = \text{Gd}$ for **1**, Tb for **2**, respectively) entity (Figure 1 and S1 in the Supporting Information). In the asymmetric unit, the nickel(II) ion in **1** and **2**, respectively, exhibits a slightly distorted octahedral coordination geometry with the equatorial positions occupied by two nitrogen and two phenoxo oxygen atoms arising from the inner compartment of the Schiff-base ligand [Ni–N = 2.011(2) and 2.053(2) Å, Ni–O = 2.036(2) and 2.021(2) Å for **1**, and Ni–N = 2.011(2) and 2.056(2) Å, Ni–O = 2.033(2) and 2.016(2)

Å for **2**, respectively], whereas the axial positions are filled by two nitrogen atoms from two coordinated MeCN molecules [Ni–N = 2.088(3) and 2.134(3) Å for **1**, and 2.090(2) and 2.133(2) Å for **2**, respectively]. The Ln(III) ion is surrounded by ten O atoms arising from the large compartment of the ligand (L) and three bidentate nitrate anions with Ln–O bond length in the range of 2.341(2)–2.653(2) Å for **1**, and 2.328(2)–2.649(2) Å for **2**, respectively. The coordination sphere of Ln^{III} is close to the staggered dodecahedron (SDD-10, D_2) for **1** and **2**, calculated using the SHAPE software (Table S6).²¹ Within the cluster, the Ni(II) and Ln(III) ions are linked to each other via two phenolate atoms with the Ni···Ln distance of 3.480(6) Å for **1** and 3.470(7) Å for **2**, the average bond angle of Ni–O–Ln is 105.20° for **1** and 105.29° for **2**, and the hinge angle (dihedral angle between the O–Ni–O and O–Ln–O planes) is 0.85° for **1** and 0.76° for **2**, respectively. The shortest intercluster M···M distance is 7.566 Å for **1**, and 7.565 Å for **2**, respectively, the neighboring clusters are linked through intermolecular C–H···O and O–H···O interactions to form three dimensional networks (Figure S2 and S3).

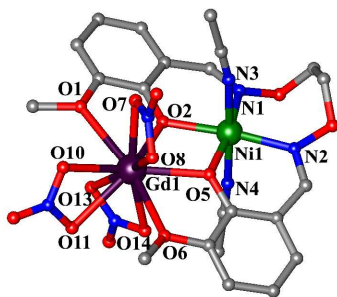


Figure 1. Perspective drawing of the crystallographically structural unit of **1** showing the atom numbering. H atoms are omitted for clarity.

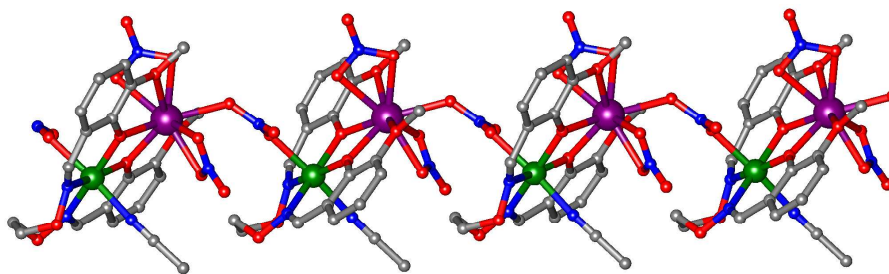


Figure 2. The one-dimensional chain structure of **3**. H atoms and one solvated acetonitrile molecule are omitted for clarity.

Complexes **3** crystallize in the monoclinic space group of Cc and made up of a neutral *anti-anti* nitrate- and phenolate-bridged infinite zigzag chain with $[-Ni-(O)_2-Dy-ONO_2-]_n$ as the repeating unit (Figure 2).

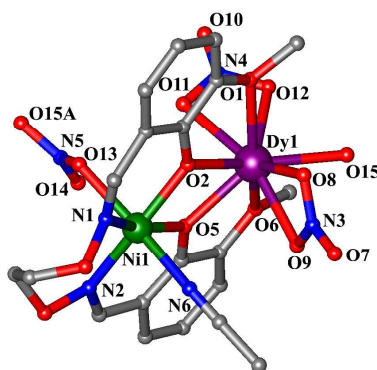


Figure 3. Perspective drawing of the crystallographically structural unit of **3** showing the atom numbering. H atoms and one solvated acetonitrile molecule are omitted for clarity.

As shown in Figure 3, the asymmetric unit of **3** consist of one neutral $[\text{Ni}(\mu\text{-L})(\text{MeCN})\text{Dy}(\text{NO}_3)_2(\mu\text{-NO}_3)]$ and one solvated acetonitrile molecule. In the Ni-Dy heterobinuclear unit, the Ni(II) ion situates in a slightly elongated octahedral surrounding with the equatorial plane occupied by N_2O_2 atoms from the ligand (L) and the two axial positions occupied by the nitrogen atom of an acetonitrile molecule and one oxygen atom of the *anti-anti* bridging nitrate ligand. The axial bond lengths (2.108(4) Å and 2.171(4) Å) are relatively longer than the equatorial ones (Ni–N = 2.023(4) and 2.037(4) Å, Ni–O = 2.010(3) and 2.005(3) Å). The Dy(III) ion is surrounded by nine oxygen atoms comprising two phenolato and two methoxy oxygen atoms from the ligand (L), four oxygen atoms arising from the two chelating nitrate anions, and the oxygen atom from the *anti-anti* bridging nitrate ligand. The Dy–O distances fall in the range 2.293(3)–2.505(4) Å. Concerning the coordination environment for the Dy(III) ion, the best description would be a spherical tricapped trigonal prism (TCTPR-9, D_{3h}). The Ni(II) and Dy(III) ions are bridged to each other via two phenolic oxygen atoms of the ligand (L) with the Ni \cdots Dy distance of 3.457 Å. The average bond angle of Ni–O–Dy is 106.90°, and the hinge angle is 8.62°. The neighboring Ni-Dy heterobinuclear units are connected to each other through the *anti-anti* bridging nitrate ligand to yield 1D infinite zigzag chain. Within a chain, all Ni-Dy heterobinuclear units have a unique orientation. The Ni-Dy distance by the nitrate bridge is 5.920 Å, which can transmit weak ferromagnetic couplings between Ni(II) and Dy(III) ions. The shortest interchain M \cdots M distance is 8.275 Å, indicating that the magnetic ions are well separated. Each chain interacts with two other adjacent

chains by H-bond interactions between the solvated and coordinated MeCN molecules, as well as bridging nitrate ligands and solvated MeCN molecules, thus forming a 2D layer (Figure S4). The layers stack into a three-dimensional (3D) structure via *Van der Waals* interactions. To our knowledge, compound **3** is unique example of 1D infinite nitrate- and phenolate-bridged Ni–Dy heterometallic chain.

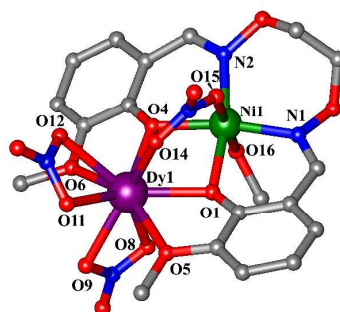


Figure 4. Perspective drawing of the crystallographically structural unit of **5** showing the atom numbering. H atoms and one solvated diethyl ether molecule are omitted for clarity.

Complex **4** and **5** are isostructural, crystallize in the triclinic P_{-1} space group and consist of one neutral Ni–Ln heterobinuclear $[\text{Ni}(\mu\text{-L})(\text{CH}_3\text{OH})(\mu\text{-NO}_3)\text{Ln}(\text{NO}_3)_2]$ ($\text{Ln} = \text{Tb}$ for **4**, and Dy for **5**, respectively) unit and one diethyl ether molecule (Figure 4 and S5). The octahedral Ni^{II} ion is axially coordinated by two oxygen atoms from a methanol molecule ($\text{Ni}\text{-O} = 2.070(3)$ Å for **4**, and $2.071(3)$ Å for **5**) and a *syn-syn* bridging nitrate ligand ($\text{Ni}\text{-O} = 2.122(2)$ Å for **4**, and $2.120(3)$ Å for **5**), and the equatorial positions are occupied by the inner compartment of the deprotonated L ligand ($\text{Ni}\text{-N} = 2.015(3)$ and $2.067(3)$ Å, $\text{Ni}\text{-O} = 2.024(2)$ and $1.999(2)$ Å for **4**, and $\text{Ni}\text{-N} = 2.029(4)$ and $2.063(4)$ Å, $\text{Ni}\text{-O} = 2.020(3)$ and $2.002(3)$ Å for **5**, respectively). The Ln^{III} ion is nine-coordinated by outer four oxygen atoms from the L ligand and four oxygen atoms from two bidentate nitrate anions, and the remaining one from the *syn-syn* bridging nitrate group with $\text{Ln}\text{-O}$ bond lengths in the range of $2.240(2)\text{-}2.548(3)$ Å for **4**, and $2.239(3)\text{-}2.542(3)$ Å for **5**, respectively. The coordination sphere of Ln^{III} in complex **4** and **5** is close to a spherical capped square antiprism (CSAPR-9, C_{4v}). Within the cluster, the distance of $\text{Ni}\cdots\text{Ln}$ is 3.348 Å for **4**, and 3.344 Å for **5**, the average bond angle of $\text{Ni}\text{-O}\text{-Ln}$ is 102.88° for **4**, and 102.50° for **5**, and the hinge angle is 13.25° for **4**, and 13.58° for **5**, respectively. The shortest intercluster $\text{M}\cdots\text{M}$ distance is 8.031 Å for **4**, and 8.046 Å for **5**. The neighboring

asymmetric unit is connected through weak C–H⋯O H-bonding and C–H⋯ π interactions to form a 3D framework (Figure S6 and S7). It is noteworthy that the binding modes of the bridging nitrate groups in complexes **3** and **5** are different. The *anti-anti* mode was displayed in **3**, whereas the *syn-syn* mode was shown in **5**. The different binding modes of bridging nitrate groups give rise to the distinct structures of **3** and **5**, then may result in their different magnetic behavior.

Magnetic Properties

The dc magnetic susceptibilities for complexes **1–5** were measured in the temperature range of 1.8–300 K under an applied magnetic fields of 1000 Oe for **1–4** and 100 Oe for **5**, respectively (Figure 5).

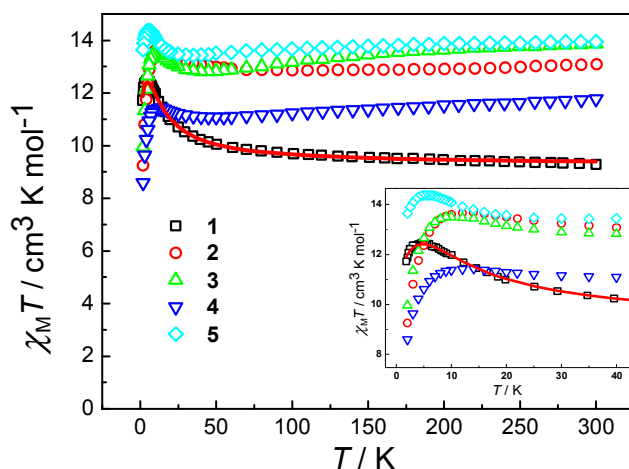


Figure 5. Temperature dependence of the $\chi_M T$ product for **1–5** under an applied magnetic fields of 1 T for **1–4** and 0.1 T for, respectively. Inset: the enlarged section of the $\chi_M T$ product for **1–5** in the low temperatures.

For **1**, the observed $\chi_M T$ value at 300 K of $9.28 \text{ cm}^3 \text{ K mol}^{-1}$ is higher than the calculated value of $8.88 \text{ cm}^3 \text{ K mol}^{-1}$ for two noninteracting Gd^{III} ($S = 7/2$) and Ni^{II} ($S = 1$) ions assuming $g = 2.0$. On cooling, the $\chi_M T$ value increases gradually before 50 K, then increases abruptly to a maximum value of $12.49 \text{ cm}^3 \text{ K mol}^{-1}$ at 4.8 K showing the predominantly ferromagnetic character, and finally decreases to $11.72 \text{ cm}^3 \text{ K mol}^{-1}$ at 1.8 K. The experimental data were analyzed on the basis of the spin-only equation derived from a spin Hamiltonian $\mathbf{H} = -J\mathbf{S}_{\text{Ni}} \cdot \mathbf{S}_{\text{Gd}}$. The best fitting is obtained with $g = 2.04$, $J = 2.62 \text{ cm}^{-1}$ and $zJ' = -0.006 \text{ cm}^{-1}$ ($R = 2.2 \times 10^{-3}$). The positive J value is coincident with the intracuster ferromagnetic interaction between Ni^{II} and Gd^{III} ions. The field dependence of the magnetization at 1.8 K increases slowly up to

$9.45N\beta$, which is close to the expected value for Ni(II) and Gd(III) ions system with ferromagnetic interaction ($S = 9/2$, Figure S8).

At room temperature, the $\chi_M T$ value per Ni^{II}Ln^{III} unit is 13.08, 13.87, 11.77 and 13.95 cm³ K mol⁻¹ for **2–5**, respectively, which are slightly deviate from the expected values of 12.82 cm³ K mol⁻¹ ($g_{Tb} = 3/2$, ⁷F₆) and 15.17 cm³ K mol⁻¹ ($g_{Dy} = 4/3$, ⁶H_{15/2}), for one uncoupled Ni^{II} (³A_{2g}, $g = 2.0$) and one Ln^{III} ion. The $\chi_M T$ product gradually descends upon cooling reaching a minimum of 12.86 cm³ K mol⁻¹ at 100 K for **2**, 12.82 cm³ K mol⁻¹ at 45 K for **3**, 11.08 cm³ K mol⁻¹ at 50 K for **4**, and 13.43 cm³ K mol⁻¹ at 35 K for **5**, respectively, likely due to the depopulation of the Ln Stark sublevels.²² Below this temperature, $\chi_M T$ increases abruptly to a maximum of 14.69 cm³ K mol⁻¹ at 14 K for **2**, 13.50 cm³ K mol⁻¹ at 10 K for **3**, 11.43 cm³ K mol⁻¹ at 14 K for **4**, and 14.37 cm³ K mol⁻¹ at 5 K for **5**, respectively. Upon further cooling, the $\chi_M T$ value decreases rapidly for **2–5**. The increase of $\chi_M T$ at low temperatures suggests that overall ferromagnetic couplings are dominated between Ni^{II} and Ln^{III} ions in **2–5**. The M vs. H curve (Figure S8) shows that the magnetization first increases steeply at the low field, and then increases slowly up to 6.62 $N\beta$ for **2**, 7.02 $N\beta$ for **3**, 5.61 $N\beta$ for **4**, and 7.22 $N\beta$ for **5**, respectively, at 50 kOe and 2 K without achieving saturation.

In order to investigate the magnetic relaxation dynamics, alternating current (ac) magnetic susceptibility measurements were performed for complexes **2–5** between 2.0–10.0 K in a 2 Oe oscillating ac field. Under a zero dc field, no signal was observed in the out-of-phase (χ'') down to 2 K for **2**, **4** and **5** (Figure S9-11).

For compound **3**, temperature- and frequency-dependent out-of-phase (χ'') signals displayed a strong frequency dependence below 6 K under zero dc field (Figure 6), indicating the existence of slow relaxation of magnetization. The relaxation time derived from the χ'' peaks follow the Arrhenius law of $\tau = \tau_0 \exp(\Delta/k_B T)$ with $\Delta/k_B = 15.8$ K, $\tau_0 = 9.26 \times 10^{-7}$ s (ac- T data, Figure 7, inset) and $\Delta/k_B = 14.4$ K, $\tau_0 = 2.10 \times 10^{-6}$ s (ac- f data, Figure S12), which is located in the normal range for SMM/SCMs.^{1–5} As the temperature is decreased, a slight curvature appears in the plot of $\ln \tau$ vs. $1/T$ derived from ac- f data, but does not become temperature independent at any point, this is due to both thermal and QTM mechanisms occurring simultaneously. The Cole–Cole diagram was fitted separately by a generalized Debye model (Figure 7).²³ The best fitting results of α values are less than 0.001, indicating a

single relaxation process mainly involved at 2.0–3.0 K.

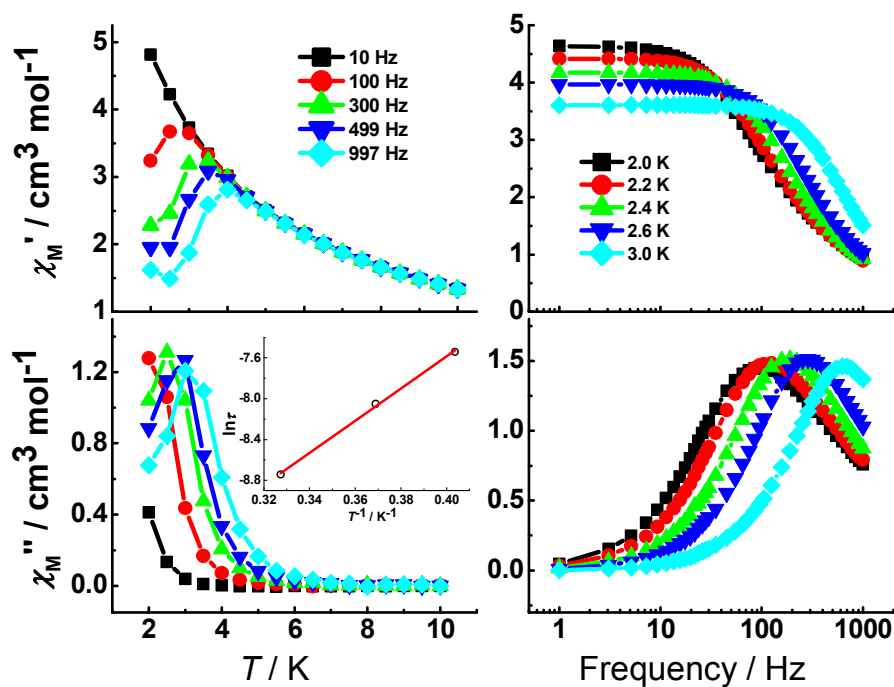


Figure 6. Temperature-dependent (left) and frequency-dependent (right) ac susceptibility for **3** under a zero applied dc field. Inset: the Arrhenius fit for the $\ln \tau$ vs T^{-1} plot from ac- T data of **3**. The red solid line represents the best fits of the data.

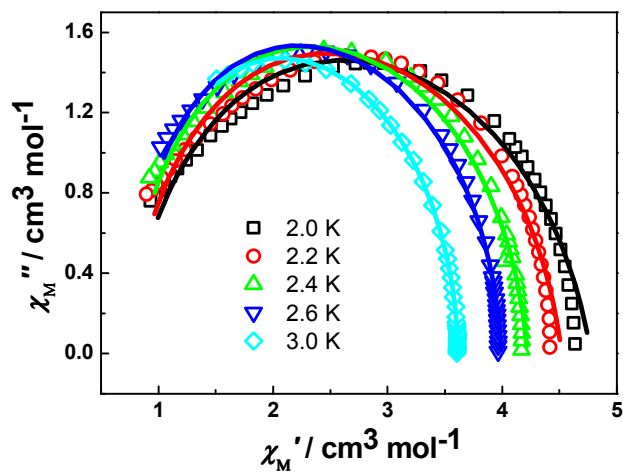


Figure 7. The Cole–Cole plots (χ'' vs. χ') of **3** at indicated temperatures. Solid lines: fit by the Debye model at corresponding colours of indicated temperatures.

In the Ising-like or anisotropic Heisenberg 1D chain models, the correlation length of ξ and χT increase exponentially with lowering temperature: $\chi T = C_{\text{eff}} \exp(\Delta_{\xi}/k_{\text{B}}T)$, where C_{eff} is the effective Curie constant and Δ_{ξ} is the energy needed to create a domain wall along the chain.^{3a,24} Thus, a linear increase of the $\ln(\chi'T)$ versus

$1/T$ plot, where χ' is the in-phase ac susceptibility measured at 10 Hz under zero dc field, would prove the magnetic one-dimensional (1D) nature and the presence of significant magnetic anisotropy. For compound **3**, $\ln(\chi'T)$ versus $1/T$ plot between 2.0 and 10 K shows a monotonous decreasing of $\ln(\chi'T)$ upon cooling (Figure S13), in conjunction with the longer Ni...Dy distance of 5.920 Å through nitrate within the chain which may transmit very weak magnetic interaction, the SCM nature of **3** can be precluded. So, **3** behaves as a SMM under zero dc field.

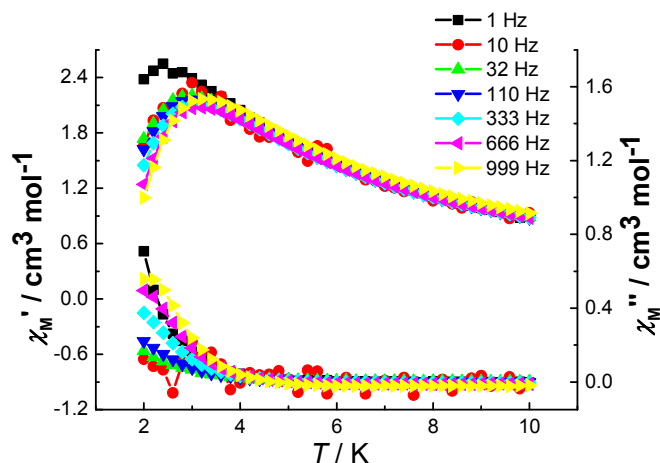


Figure 8. Temperature dependence of the in-phase χ' and out-of-phase χ'' at different frequencies in a 2 Oe ac field oscillating at 1–999 Hz with 2000 Oe dc field for **5**.

While the 2000 Oe dc field was added, compound **5** exhibited a frequency-dependent χ'' signal below 4 K (Figure 8). Unfortunately, no peaks were found at frequencies lower than 999 Hz until 2.0 K due to the fast QTM, which impeded confirmation of SMM-type behavior. Compared with the single-molecule magnet behavior of **3** under zero dc field, **5** only displays slow magnetic relaxation under 2000 Oe dc field. It has been illustrated that the single axial ligand-field symmetry around Ln^{III} ions is of great importance in determining single axial magnetic anisotropy of the entire molecule.^{16a, 25} The Dy^{III} ion in **3** located in D_{3h} local symmetry, C_{4v} in **5**. The higher local symmetry (D_{3h}) of Dy^{III} ion decreasing the QTM, as well as the unique orientation of Ni^{II} and Dy^{III} ions within the 3D structure, is responsible for the exhibition of SMM behavior under zero dc field in **3**.

Conclusion

In summary, we reported several double/triply bridged $\text{Ni}^{\text{II}}\text{-Ln}^{\text{III}}$ heterodinuclear and one-dimensional complexes. In particular, compound **3** displays a rare nitrate-

and phenolate-bridged Ni–Dy heterometallic chain structure. All complexes show ferromagnetic interaction between Ni^{II} and Ln^{III} ions, **3** behaves as single-molecule magnet with effective energy of 15.8 K under zero dc field, however, **5** only displays the slow magnetic relaxation under 2000 Oe dc field. The differences from the binding modes of bridging nitrate groups in **3** and **5** result in the distinct structures which change the symmetry of the ligand-field of Dy^{III} ions and affect the quantum tunnelling of magnetization, and then lead to the different magnetic behavior. Further experimental and theoretical work towards improving the effective energy of 3d-4f spincarrier single-molecule/single-chain magnets by introducing metal-cyanide building block is under way.

Acknowledgments

This work was supported by the Major State Basic Research Development Program (2011CB808704), the National Natural Science Foundation of China (21021062, 91022031, 21171092 and 21401101) and the Natural Science Foundation of Jiangsu Province (BK20140935).

Supporting Information

Additional structure and magnetic characterization data, and X-ray crystallographic files in CIF format for **1–5**.

References

- (a) D. Gatteschi, R. Sessoli and J. Villain, *Molecular Nanomagnets*, Oxford University Press, Oxford, 2006, p. 141; (b) J. S. Miller and D. Gatteschi, *Chem. Soc. Rev.*, 2011, **40**, 3065 and references in the issue; (c) J. M. Clemente-Juan, E. Coronado and A. Gaita-Ariño, *Chem. Soc. Rev.*, 2012, **41**, 7464.
- (a) I.-R. Jeon and R. Clérac, *Dalton Trans.*, 2012, 9569; (b) H. Miyasaka, M. Julve, M. Yamashita and R. Clérac, *Inorg. Chem.*, 2009, **48**, 3420; (c) K. Bernot, J. Luzon, R. Sessoli, A. Vindigni, J. Thion, S. Richeter, D. Leclercq, J. Larionova and A. Van der Lee, *J. Am. Chem. Soc.*, 2008, **130**, 1619; (d) T.-T. Wang, M. Ren, S.-S. Bao, B. Liu, L. Pi, Z.-S. Cai, Z.-H. Zheng, Z.-L. Xu and L.-M. Zheng, *Inorg. Chem.*, 2014, **53**, 3117.

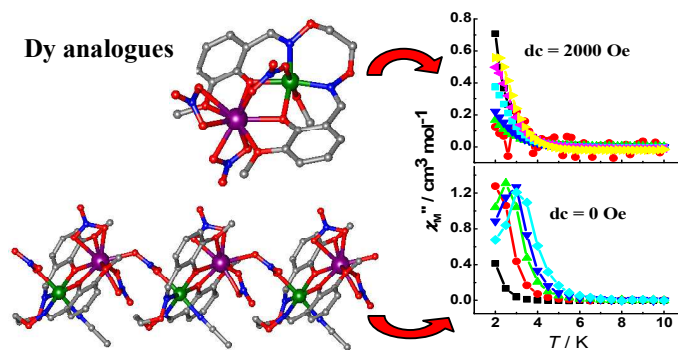
- 3 (a) C. Coulon, H. Miyasaka and R. Clérac, *Struct. Bonding*, 2006, **122**, 163; (b) R. J. Glauber, *J. Math. Phys.*, 1963, **4**, 294; (c) W. X. Zhang, R. Ishikawa, B. Breedlove and M. Yamashita, *RSC Adv.*, 2013, **3**, 3772; (d) J. Ru, F. Gao, T. Wu, M.-X. Yao, Y.-Zh. Li and J.-L. Zuo, *Dalton Trans.*, 2014, 933; (e) G. Aromi and E. K. Brechin, *Struct. Bonding*, 2006, **122**, 1; (f) D. Gatteschi and R. Sessoli, *Angew. Chem., Int. Ed.*, 2003, **42**, 268; (g) C. F. Wang, D. P. Li, X. Chen, X. M. Li, Y. Z. Li, J. L. Zuo, X. Z. You, *Chem. Commun.*, 2009, 6940.
- 4 (a) J. R. Friedman, M. P. Sarachik, J. Tejada and R. Ziolo, *Phys. Rev. Lett.*, 1996, **76**, 3830; (b) L. Thomas, F. Lioni, R. Ballou, D. Gatteschi, R. Sessoli and B. Barbara, *Nature*, 1996, **383**, 145; (c) W. Wernsdorfer, R. Clérac, C. Coulon, L. Lecren and H. Miyasaka, *Phys. Rev. Lett.*, 2005, **95**, 237203.
- 5 (a) L. Bogani and W. Wernsdorfer, *Nat. Mater.*, 2008, **7**, 179; (b) M. N. Leuenberger and D. Loss, *Nature*, 2001, **410**, 789.
- 6 S. Osa, T. Kido, N. Matsumoto, N. Re, A. Pochaba, J. Mrozinski, *J. Am. Chem. Soc.* 2003, **126**, 420.
- 7 (a) R. Sessoli, A. K. Powell, *Coord. Chem. Rev.* 2009, **253**, 2328; (b) O. Kahn, *Acc. Chem. Res.* 2000, **33**, 647; (c) R. E. P. Winpenny, *Chem. Soc. Rev.* 1998, **27**, 447; (d) O. Kahn, J. Galy, Y. Journaux, *J. Am. Chem. Soc.* 1982, **104**, 2165; (e) Y. Pei, M. Verdager, O. Kahn, J. Sletten, J.-P. Renard, *J. Am. Chem. Soc.* 1986, **108**, 428; (f) D. N. Woodruff, R. E. P. Winpenny, R. A. Layfield, *Chem. Rev.* 2013, **113**, 5110.
- 8 (a) C. Benelli, D. Gatteschi, *Chem. Rev.* 2002, **102**, 2369; (b) R. Sessoli, A. K. Powell, *Coord. Chem. Rev.* 2009, **253**, 2328; (c) L. Sorace, C. Benelli, D. Gatteschi, *Chem. Soc. Rev.* 2011, **40**, 3092.
- 9 (a) M. Andruh, J. P. Costes, C. Diaz, S. Gao, *Inorg. Chem.* 2009, **48**, 3342; (b) G. E. Kostakis, I. J. Hewitt, A. M. Ako, V. Mereacre, A. K. Powell, *Philos. Trans. R. Soc., A* 2010, **368**, 1509; (c) M. Andruh, *Chem. Commun.* 2011, **47**, 3025; (d) M.-G. Alexandru, D. Visinescu, A. M. Madalan, F. Lloret, M. Julve, M. Andruh, *Inorg. Chem.* 2012, **51**, 4906.
- 10 (a) C. Aronica, G. Pilet, G. Chastanet, W. Wernsdorfer, J.-F. Jacquot, D. Luneau, *Angew. Chem., Int. Ed.* 2006, **45**, 4659; (b) G. J. Sopasis, A. B. Canaj, A. Philippidis, M. Siczek, T. Lis, J. R. O'Brien, M. M. Antonakis, S. A. Pergantis, C. J. Milios, *Inorg. Chem.* 2012, **51**, 5911; (c) T. Shiga, H. Miyasaka, M. Yamashita, M. Morimoto, M. Irie, *Dalton Trans.* 2011, 2275; (d) H. L. C. Feltham, R. Clérac,

- A. K. Powell, S. Brooker, *Inorg. Chem.* 2011, **50**, 4232; (e) V. Baskar, K. Gopal, M. Helliwell, F. Tuna, W. Wernsdorfer, R. E. P. Winpenny, *Dalton Trans.* 2010, **39**, 4747; (f) K. C. Abhijeet, J. Biplab, R. Eric, R. Guillaume, K. G. Sujit, *Inorg. Chem.* 2012, **51**, 9159.
- 11 (a) C. M. Zaleski, E. C. Depperman, J. W. Kampf, M. L. Kirk, V. L. Pecoraro, *Angew. Chem., Int. Ed.* 2004, **43**, 3912; (b) G. Karotsis, S. Kennedy, S. J. Teat, C. M. Beavers, D. A. Fowler, J. J. Morales, M. Evangelisti, S. J. Dalgarno, E. K. Brechin, *J. Am. Chem. Soc.* 2010, **132**, 12983; (c) A. Saha, M. Thompson, K. A. Abboud, W. Wernsdorfer, G. Christou, *Inorg. Chem.* 2011, **50**, 10476; (d) A. M. Ako, V. Mereacre, R. Clérac, W. Wernsdorfer, I. J. Hewitt, C. E. Anson, A. K. Powell, *Chem. Commun.* 2009, 544; (e) Q.-W. Xie, A.-L. Cui, J. Tao, H.-Z. Kou, *Dalton Trans.* 2012, **41**, 10589; (f) J. Y. Liu, C. B. Ma, H. Chen, M. Q. Hu, H. M. Wen, H. H. Cui, X. W. Song, C. N. Chen, *Dalton Trans.* 2013, **42**, 2423.
- 12 (a) Q. Zhou, F. Yang, D. Liu, Y. Peng, G. H. Li, Z. Shi, S. H. Feng, *Dalton Trans.* 2013, **42**, 1039; (b) G.-F. Xu, P. Gamez, J. Tang, R. Clérac, Y.-N. Guo, Y. Guo, *Inorg. Chem.* 2012, **51**, 5693; (c) D. Schray, G. Abbas, Y. Lan, V. Mereacre, A. Sundt, J. Dreiser, O. Waldmann, G. E. Kostakis, C. E. Anson, A. K. Powell, *Angew. Chem., Int. Ed.* 2010, **49**, 5185; (d) Y.-F. Zeng, G.-C. Xu, X. Hu, Z. Chen, X.-H. Bu, S. Gao, E. C. Sañudo, *Inorg. Chem.* 2010, **49**, 9374; (e) S. Schmidt, D. Prodius, G. Novitchi, V. Mereacre, G. E. Kostakis, A. K. Powell, *Chem. Commun.* 2012, 9825.
- 13 (a) V. Chandrasekhar, B. M. Pandian, J. J. Vittal, R. Clérac, *Inorg. Chem.* 2009, **48**, 1148; (b) K. C. Mondal, A. Sundt, Y. Lan, G. E. Kostakis, O. Waldmann, L. Ungur, L. F. Chibotaru, C. E. Anson, A. K. Powell, *Angew. Chem., Int. Ed.* 2012, **51**, 7550; (c) S. K. Langley, N. F. Chilton, L. Ungur, B. Moubaraki, L. F. Chibotaru, K. S. Murray, *Inorg. Chem.* 2012, **51**, 11873; (d) L. Ungur, M. Thewissen, J.-P. Costes, W. Wernsdorfer, and L. F. Chibotaru, *Inorg. Chem.* 2013, **52**, 6328.
- 14 (a) V. Chandrasekhar, P. Bag, W. Kroener, K. Gieb, and P. Müller, *Inorg. Chem.* 2013, **52**, 13078; (b) N. Ahmed, C. Das, S. Vaidya, S. K. Langley, K. S. Murray, and M. Shanmugam, *Chem. –Eur. J.* 2014, **20**, 14235; (c) M. K. Chandra, G. E. Kostakis, Y. Lan, W. Wernsdorfer, C. E. Anson, A. K. Powell, *Inorg. Chem.* 2011, **50**, 11604; (d) Y. Gao, L. Zhao, X. Xu, G.-F. Xu, Y.-N. Guo, J. Tang, Z. Liu,

- Inorg. Chem.* 2011, **50**, 1304; (e) L. Zhao, J. f. Wu, H.-sh. Ke, and J. k. Tang, *Inorg. Chem.* 2014, **53**, 3519.
- 15 (a) D. Visinescu, A. M. Madalan, M. Andruh, C. Duhayon, J.-P. Sutter, L. Ungur, W. V. d. Heuvel, L. F. Chibotaru, *Chem. Eur. J.* 2009, **15**, 11808; (b) R. Gheorghe, A. M. Madalan, J.-P. Costes, W. Wernsdorfer, M. Andruh, *Dalton Trans.*, 2010, **39**, 4734; (c) K.-Q. Hu, X. Jiang, Sh.-Q. Wu, C.-M. Liu, A.-L. Cui, and H.-Zh. Kou, *Inorg. Chem.* 2015, **54**, 1206; (d) M.-X. Yao, Q. Zheng, K. Qian, Y. Song, S. Gao, J.-L. Zuo, *Chem. -Eur. J.* 2013, **19**, 294; (e) M. Zhu, P. Hu, Y. g. Li, X. f. Wang, L. c. Li, D. zh. Liao, V. M. L. D. P. Goli, S. Ramasesha, and J.-P. Sutter, *Chem. -Eur. J.* 2014, **20**, 13356.
- 16 (a) J. Liu, Y.-C. Chen, Z.-X. Jiang, J.-L. Liu, J.-H. Jia, L.-F. Wang, Q.-W. Li and M.-L. Tong, *Dalton Trans.*, 2015, **44**, 8150; (b) J.-L. Liu, J.-Y. Wu, Y.-C. Chen, V. Mereacre, A. K. Powell, L. Ungur, L. F. Chibotaru, X.-M. Chen, and M.-L. Tong, *Angew. Chem. Int. Ed.* 2014, **53**, 12966; (c) S. K. Langley, D. P. Wielechowski, V. Vieru, N. F. Chilton, B. Moubaraki, B. F. Abrahams, L. F. Chibotaru, K. S. Murray, *Angew. Chem. Int. Ed.* 2013, **52**, 12014; (d) Y.-N. Guo, G.-F. Xu, W. Wernsdorfer, L. Ungur, Y. Guo, J. Tang, H.-J. Zhang, L. F. Chibotaru, A. K. Powell, *J. Am. Chem. Soc.* 2011, **133**, 11948; (e) F. Habib, P.-H. Lin, J. Long, I. Korobkov, W. Wernsdorfer, M. Murugesu, *J. Am. Chem. Soc.* 2011, **133**, 8830.
- 17 (a) S. Akine, T. Taniguchi, W. k. Dong, S. Masubuchi and T. Nabeshima, *J. Org. Chem.* 2005, **70**, 1704; (b) A. Shigehisa, M. Takashi, T. Takanori, and N. Tatsuya, *Inorg. Chem.* 2005, **44**, 3270; (c) T. D. Pasatoiu, J.-P. Sutter, A. M. Madalan, F. Z. C. Fella, C. Duhayon, M. Andruh, *Inorg. Chem.*, 2011, **50**, 5890.
- 18 *SAINT-Plus*, version 6.02, Bruker Analytical X-ray System: Madison, WI, 1999.
- 19 G. M. Sheldrick *SADABS* An empirical absorption correction program. Bruker Analytical X-ray Systems: Madison, WI, 1996.
- 20 G. M. Sheldrick *SHELXTL-2013*, Universität of Göttingen: Göttingen, Germany, 2013.
- 21 Llunell, M.; Casanova, D.; Cirera, J.; Alemany, P.; Alvarez, S. *SHAPE*, version 2.1; Barcelona, Spain, 2013.
- 22 (a) T. D. Pasatoiu, J.-P. Sutter, A. M. Madalan, F. Z. C. Fella, C. Duhayon, M. Andruh, *Inorg. Chem.* 2011, **50**, 5890; (b) T. D. Pasatoiu, M. Etienne, A. M. Madalan, M. Andruh, R. Sessoli, *Dalton Trans.*, 2010, 4802; (c) T. Shiga, N. Ito,

- A. Hidaka, H. Okawa, S. Kitagawa, M. Ohba, *Inorg. Chem.* 2007, **46**, 3492.
- 23 M. Hagiwara, *J. Magn. Magn. Mater.*, 1998, **89**, 177.
- 24 (a) J. M. Loveluck, S. W. Lovesey, S. Aubry, *J. Phys. C: Solid State Phys.* 1975, **8**, 3841; (b) K. Nakamura, T. Sasada, *J. Phys. C: Solid State Phys.* 1978, **11**, 331; (c) H. Miyasaka, M. Julve, M. Yamashita, R. Clérac, *Inorg. Chem.* 2009, **48**, 3420.
- 25 (a) J.-L. Liu, J.-Y. Wu, Y.-C. Chen, V. Mereacre, A. K. Powell, L. Ungur, L. F. Chibotaru, X.-M. Chen, and M.-L. Tong, *Angew. Chem. Int. Ed.* 2014, **53**, 12966; (b) G.-J. Chen, Y.-N. Guo, J.-L. Tian, J. k. Tang, W. Gu, X. Liu, Sh.-P. Yan, P. Cheng, and D.-Zh. Liao, *Chem. –Eur. J.* 2012, **18**, 2484.

GRAPHIC ABSTRACT



By using the Salen-type ligand and changing reaction solvent, series of Ni^{II} - Ln^{III} complexes have been obtained and structurally and magnetically characterized.